DanceHMR: Hand-Aware Whole-Body Human Mesh Recovery from Monocular Videos

WENHAO SHEN*, ByteDance, China
MING ZHOU*†, ByteDance, China
HENGYUAN ZHANG, ByteDance, China
SIYUAN BIAN, ByteDance, China
YOUJIANG XU, ByteDance, China
YUAN ZHANG, ByteDance, China

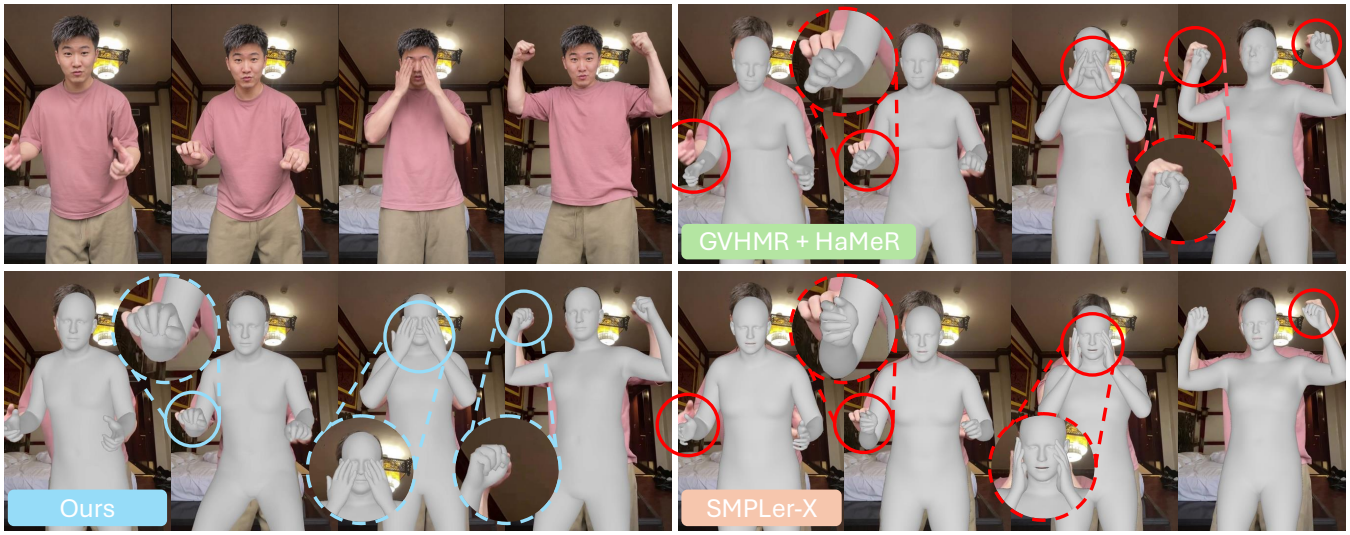

Fig. 1. Given a monocular internet video, our method reconstructs temporally coherent and 2D consistent whole-body motion. Previous video-based HMR methods focus predominantly on the body; when combined with hand models (e.g., GVHMR [Shen et al. 2024a] + HaMeR [Pavlakos et al. 2024]), they often produce unnatural wrist orientations and temporal inconsistencies. Image-based whole-body models such as SMPLer-X [Cai et al. 2024] process frames independently, and the hands are often too small to recover reliable articulation, leading to inaccurate and jittery hand motion. By modeling the body and hands together, our approach produces temporally stable hand articulation and fluid whole-body dynamics.

Monocular video human mesh recovery is essential for digital humans, avatar animation, and embodied simulation, where both temporal stability and expressive whole-body motion are required. Existing video HMR methods produce coherent body motion but often overlook detailed hand articulation, while image-based whole-body methods recover SMPL-X meshes independently per frame, often leading to jittery and inaccurate hand motion. We present a temporally coherent whole-body HMR framework for challenging in-the-wild monocular videos. Our model unifies body context and part-specific hand observations through residual body-hand fusion, enabling stable body motion and detailed hand recovery within a single temporal architecture. We further introduce close-up-aware augmentation to improve robustness under upper-body framing. Experiments on whole-body and body-only benchmarks demonstrate improved hand reconstruction and competitive body accuracy. Our method also produces temporally stable and 2D-consistent SMPL-X motion in challenging real-world videos.

CCS Concepts: • **Computing methodologies** → **Motion capture**.

Additional Key Words and Phrases: Human mesh recovery

ACM Reference Format:
Wenhao Shen, Ming Zhou, Hengyuan Zhang, Siyuan Bian, Youjiang Xu, and Yuan Zhang. 2026. DanceHMR: Hand-Aware Whole-Body Human Mesh Recovery from Monocular Videos. In *SIGGRAPH Asia 2026 Conference Papers (SA Conference Papers '26), December 01–04, 2026, Kuala Lumpur, Malaysia.* ACM, New York, NY, USA, 11 pages. https://doi.org/10.1145/3829340.3842190

*Both authors contributed equally to this research.
†Corresponding author.

Authors' Contact Information: Wenhao Shen, ByteDance, Shenzhen, China, wenhao005@e.ntu.edu.sg; Ming Zhou, ByteDance, Shenzhen, China, zhouming.9527@bytedance.com; Hengyuan Zhang, ByteDance, Shenzhen, China, hengyuan.zhang@stu.pku.edu.cn; Siyuan Bian, ByteDance, Shenzhen, China, siyuanb@umich.edu; Youjiang Xu, ByteDance, Shenzhen, China, xuyoujiang.01@bytedance.com; Yuan Zhang, ByteDance, Shenzhen, China, zhang.yuan09@gmail.com.

This work is licensed under a Creative Commons Attribution 4.0 International License.
SA Conference Papers '26, Kuala Lumpur, Malaysia
© 2026 Copyright held by the owner/author(s).
ACM ISBN 979-8-4007-2842-6/2026/12
https://doi.org/10.1145/3829340.3842190

1 Introduction

Monocular human mesh recovery (HMR) from videos is a foundational technology for scalable human digitization, serving industrial applications such as motion generation data acquisition, avatar animation, and embodied AI. For these downstream systems, temporal coherence is essential; frame-wise jitter or physical discontinuity renders the extracted motion unusable for training pipelines or physical simulation. Furthermore, in real-world scenarios like livestreaming, dancing, and human-object interaction, hands are central to conveying motion semantics and visual realism. Recovering accurate, expressive, and temporally stable articulations for both the body and hands jointly is therefore a critical challenge.

Recent video HMR methods [Chen et al. 2025; Li et al. 2025; Shen et al. 2024a; Shin et al. 2024; Wang et al. 2026; Yin et al. 2024] stabilize body motion but typically neglect detailed hand articulation. Therefore, they are insufficient for close-up and hand-centric videos where precise finger motion and wrist-body consistency are important. A straightforward solution is to combine a video-based body estimator with a hand reconstruction model. However, the independent estimation of the body and hands usually leads to physically disjointed wrist orientations. Moreover, hand self-occlusion, blur and partial visibility are common in real-world videos, making image-based hand predictions prone to severe jitter and implausible poses.

Another challenge comes from the camera composition of real-world videos. Many internet videos are not captured as standard full-body sequences found in typical motion capture benchmarks. Livestream, vlog, and speech videos heavily feature close-up or upper-body framing, with hands frequently moving in and out of the image boundaries. Existing models trained predominantly on full-body crops suffer from a severe distribution gap in these scenarios, leading to inaccurate body-to-image alignment, distorted head projections, and unstable pose estimates.

These observations motivate a simple but important design principle: body motion, hand articulation, and temporal context should be modeled jointly rather than independently. The body pose provides strong spatial and anatomical constraints for wrist orientation and general hand placement, while focused hand crops and 2D keypoints provide complementary local evidence for complex finger articulation. Furthermore, temporal context is essential to infer plausible hand poses when visual observations of the extremities are noisy, blurred, truncated, or temporarily missing.

In this paper, we present a temporally coherent whole-body HMR framework designed for challenging in-the-wild monocular videos. Given a video sequence, our model jointly predicts body and hand parameters in a unified temporal architecture. It integrates part-specific observations through a hand-aware temporal transformer. Instead of directly stitching hand pose constraints from an image-based hand model, we encode hand visual features and explicit 2D hand geometry with independent left- and right-hand branches. The encoded hand evidence is then injected as residual refinements into a body-anchored temporal representation. This acts as a set of complementary soft observations, allowing the model to adaptively utilize reliable visual cues when hands are visible, and rely on temporal context and geometric priors when they are occluded.

To bridge the gap between benchmark-style full-body data and real-world close-up videos, we introduce a truncation-aware training strategy. By simulating temporally consistent half-body crops from existing datasets, we expose the network to diverse partial-body framing and hand entry/exit events. We train the model in a two-stage curriculum: first learning broad temporal body and hand motion priors from mixed-quality data, and subsequently emphasizing high-quality hand data and distal fingertip supervision to refine fine-grained hand articulation.

Extensive experiments show that DanceHMR improves hand reconstruction and temporal stability with a lightweight trainable model. This efficiency is enabled by reusing strong frozen body and hand visual priors and focuses on part-specific fusion and temporal reasoning. Close-up-aware augmentation and hand-focused training further improve robustness to unreliable hand observations.

In summary, our main contributions are:

- We propose DanceHMR, a temporally coherent whole-body HMR framework that recovers stable body and hand motion from monocular videos.
- We propose a close-up-aware augmentation strategy for upper-body and truncated videos, improving robustness in challenging real-world scenarios such as vlog, livestream, and hand-centric videos.
- Extensive experiments demonstrate that our method substantially improves hand reconstruction accuracy and temporal stability over existing whole-body methods.

2 Related Work

2.1 Image-Based Whole-Body and Hand Mesh Recovery

Recent image-based human mesh recovery methods [Cai et al. 2024; Goel et al. 2023; Shen et al. 2026, 2025; Wu et al. 2026; Yin et al. 2026] extend monocular HMR to expressive SMPL-X estimation. ExPose [Choutas et al. 2020] and PIXIE [Feng et al. 2021] combine part-specific body, hand, and face experts to improve local reconstruction quality. PyMAF-X [Zhang et al. 2023] separately refines body and hand predictions through mesh-aligned feedback and relies on post-hoc integration. More recent methods [Cai et al. 2024; Lin et al. 2023; Shen et al. 2024b; Yin et al. 2026] further improve large-scale expressive human reconstruction with stronger transformer backbones, scalable training strategies, or adaptation mechanisms. These methods achieve impressive per-frame reconstruction quality and serve as strong baselines for body and hand mesh recovery. However, they are primarily designed for individual images and therefore do not explicitly enforce temporal consistency when applied frame-by-frame to videos.

Beyond whole-body mesh recovery, recent works also focus on monocular hand reconstruction. HaMeR [Pavlakos et al. 2024] reconstructs detailed 3D hand meshes with transformer-based image modeling, while WiLoR [Potamias et al. 2025] further improves in-the-wild hand localization and reconstruction robustness. More recent methods such as HaWoR [Zhang et al. 2025] extend hand reconstruction toward world-referenced hand motion recovery from monocular videos. These methods achieve strong per-frame hand reconstruction quality when hands are clearly visible. However, directly stitching independently estimated hands onto a video body

sequence often leads to unstable hand motion and wrist inconsistency. In contrast, we fuse hand evidence into a body-anchored representation before temporal reasoning for coherent whole-body mesh recovery.

2.2 Video Human Mesh Recovery

Video HMR methods address the temporal inconsistency of image-based regressors by exploiting motion context across frames. Early video HMR methods [Choi et al. 2021; Kocabas et al. 2020; Rempe et al. 2021; Shen et al. 2023; Wei et al. 2022] mainly improve temporal body consistency through temporal dynamics modeling and motion-prior regularization. Later works [Goel et al. 2023; Sun et al. 2023; Ye et al. 2023; Yuan et al. 2022] extend this line toward video-level tracking and global motion recovery under dynamic cameras. However, their output space and evaluation focus are still largely body-centric. They mainly target SMPL body motion rather than detailed hand articulation, wrist-body consistency, or robust body and hand recovery in close-up and truncated videos.

Another line of work improves world-grounded video HMR. WHAM [Shin et al. 2024] introduces a body motion recovery framework that combines video features, camera motion, and contact-aware refinement. TRAM [Wang et al. 2024] estimates global human trajectory and local body motion by combining SLAM-based camera motion estimation with a video transformer. GVHMR [Shen et al. 2024a] further formulates global motion recovery in gravity-view coordinates to reduce camera-motion ambiguity. WHAC [Yin et al. 2024] and Human3R [Chen et al. 2025] also explore expressive or scene-aware video reconstruction in world coordinates. In parallel, PromptHMR-Vid [Wang et al. 2025], DUOMO [Wang et al. 2026], and GENMO [Li et al. 2025] investigate promptable or generative formulations for video human motion recovery, introducing stronger temporal and motion priors for ambiguous observations. These methods significantly advance video-based human motion recovery, especially in temporal stability and global trajectory estimation. Despite these advances, existing video HMR methods still mainly focus on body motion and global reconstruction, while detailed and temporally coherent hand recovery remains under-explored. Our work addresses this gap by extending temporal whole-body recovery to articulated hands under noisy, occluded, or truncated real-world observations.

3 Method

3.1 Method Overview

Given a monocular video sequence $\mathcal{I}_{1:T} = \{I_t\}_{t=1}^{T}$, our goal is to recover a temporally coherent SMPL-X motion sequence including body pose, hand articulation, camera-space translation, gravity-aware global motion, and contact states. For each frame, we extract frame-aligned observations $C_t = \{C_t^b, C_t^{lh}, C_t^{rh}\}$. The body observation $C_t^b = \{K_t^b, F_t^b, B_t^b, \Omega_t\}$ consists of body 2D keypoints K_t^b, body crop features F_t^b, a camera-aware body-box token B_t^b, and camera angular velocity Ω_t. Similarly, the left- and right-hand observations $C_t^{lh} = \{K_t^{lh}, F_t^{lh}, B_t^{lh}\}$ and $C_t^{rh} = \{K_t^{rh}, F_t^{rh}, B_t^{rh}\}$ contain hand 2D keypoints, hand crop features, and camera-aware hand-box tokens.

Our architecture follows a body-centric but hand-aware design. We first encode body observations into a stable per-frame token. Left and right hand observations are encoded separately as part-specific hand evidence and fused into a residual hand vector, which is injected into the body token before temporal modeling. The fused token sequence is processed by a temporal motion encoder and decoded into a coupled camera-gravity SMPL-X representation $\mathbf{x}_{1:T}$. To improve robustness in real-world videos, we further introduce a close-up-aware training strategy that exposes the model to partially visible body and hand observations, such as close-up views and hands entering or leaving the image. During inference, we optionally apply a physically grounded trajectory refinement step to reduce foot sliding and stabilize global motion.

3.1.1 Camera-gravity SMPL-X representation. Existing video HMR methods commonly represent human motion in the camera coordinate system, which facilitates image alignment and 2D reprojection supervision. However, relying solely on camera-space motion makes it difficult to maintain temporally stable motion under moving cameras. Following the gravity-view coordinate system [Shen et al. 2024a], we adopt a coupled representation that jointly models camera-aligned human motion and gravity-aware motion cues. Different from previous body-centric representations, we extend the representation to SMPL-X and explicitly model articulated hands.

Specifically, for each frame t, the global motion component consists of the gravity-view orientation $\Gamma_t^{GV} \in \mathbb{R}^6$ and the local root velocity $\mathbf{v}_t^{root} \in \mathbb{R}^3$. The local human pose is represented by the full SMPL-X pose rotations $\theta_t^x \in \mathbb{R}^{55\times3}$, which include body joints, hands, jaw, and eye poses. We also include the shape parameters $\beta_t \in \mathbb{R}^{10}$. To preserve image-space alignment, we include the camera-space human trajectory, consisting of the camera-frame orientation Γ_t^c and translation τ_t^c. Additionally, we predict static-contact states $\mathbf{p}_t$ for selected foot and wrist joints, which provide cues for global trajectory refinement.

The complete motion sequence is denoted as $\mathbf{x}_{1:T} = \{\mathbf{x}_t\}_{t=1}^{T}$, where each frame-level motion representation is defined as

$$\mathbf{x}_t = \left(\Gamma_t^{GV}, \mathbf{v}_t^{root}, \theta_t^x, \beta_t, \Gamma_t^c, \tau_t^c, \mathbf{p}_t\right). \tag{1}$$

This representation combines camera-aligned reconstruction with gravity-aware motion cues. The camera-space components enable direct supervision from image observations, while the gravity-view orientation and root velocity improve temporal motion stability under moving cameras. By explicitly modeling articulated hands in SMPL-X, our model preserves wrist-hand consistency.

3.2 Hand-Aware Whole-Body Motion Model

3.2.1 Body-anchored frame tokens. We first construct a body-centric frame token to aggregate the global human context. To achieve this, we combine explicit geometric constraints from 2D keypoints with the appearance features of the body crop. We also incorporate a camera-aware bounding-box token B_t^b, which encodes the box center and scale normalized by the focal length, thereby preserving the subject's location and size in the full image. The camera angular velocity Ω_t is obtained by converting the relative 6D rotation between adjacent frames, providing an explicit cue for disentangling camera egomotion from human motion. These distinct observation streams are projected into a shared latent space and fused additively to form

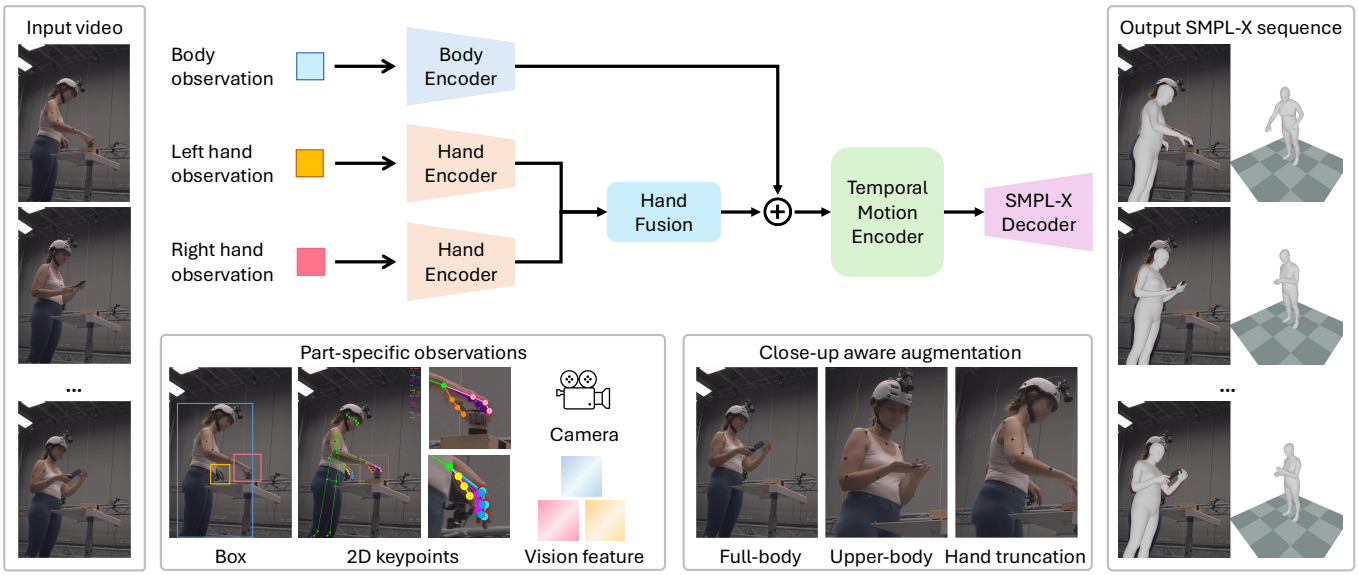

Fig. 2. Framework overview. Given an input monocular video, we separately encode part-specific body and hand observations. Hand evidence is fused into the body representation as residual cues before temporal modeling. A temporal motion encoder then reconstructs temporally coherent SMPL-X motion sequences. During training, we additionally employ close-up-aware augmentation to improve robustness for upper-body views and hand truncation scenarios.

the body token z_t^b:

$$z_t^b = E_K^b(K_t^b) + E_F^b(F_t^b) + E_B^b(B_t^b) + E_\Omega(\Omega_t). \tag{2}$$

The body token provides a robust global context for the entire person. Since hand location and wrist orientation are strongly constrained by the upper body, shoulder, elbow, and global body pose, we use the body token as the central representation into which hand evidence is subsequently injected.

3.2.2 Part-specific hand tokens. In parallel, we encode left and right hand tokens using part-specific streams:

$$z_t^h = E_K^h(K_t^h) + E_F^h(F_t^h) + E_B^h(B_t^h), \quad h \in \{lh, rh\}. \tag{3}$$

The hand crop feature preserves fine visual details that are often lost in the body crop, while the hand keypoints and hand-box token provide explicit geometric evidence about finger layout, hand location, and scale. The left and right hand observations are encoded separately before fusion, preventing detailed hand information from being overwhelmed by the stronger body signal.

For keypoint observations, we use confidence-aware encoding. Visible joints are embedded from their 2D coordinates via a linear projection, while low-confidence joints are replaced by learned missing-joint embeddings. This allows the network to retain the identity of missing joints without trusting unreliable detector coordinates. The same principle is applied to body and hand keypoints, utilizing separate encoders for the body, left hand, and right hand.

Crucially, the hand streams are not independent hand predictors; they are local evidence encoders whose outputs are injected into the shared body-hand temporal representation.

3.2.3 Residual body-hand fusion. We inject hand evidence into the body-centric representation through a residual fusion design. The left and right hand tokens are concatenated and projected by an individual hand fusion MLP, denoted as ϕ_h. The resulting hand evidence vector is added to the body token before temporal modeling:

$$z_t = z_t^b + \phi_h\left([z_t^{lh}, z_t^{rh}]\right). \tag{4}$$

This design avoids two common failure modes: directly compressing whole-body observations through a single encoder can dilute fine hand details, while post-hoc stitching of hands and body predictions struggles with wrist-body consistency. By injecting hand evidence before temporal reasoning, the model jointly refines body pose, wrist orientation, and hand articulation.

Unlike early fusion by aggregating all observations, our residual fusion preserves the body representation as the main temporal carrier and treats hand evidence as a structured refinement. The residual formulation also improves robustness. When hand observations are unreliable, the body token provides a stable motion prior. With reliable hand evidence, the residual branch injects local hand details into the temporal model. This is particularly important for close-up videos, motion blur, and partial hand visibility.

The fused frame tokens are finally processed by a temporal motion encoder, which propagates information across frames and produces contextualized motion features $h_{1:T}$:

$$h_{1:T} = \mathcal{T}(z_{1:T}). \tag{5}$$

We use relative temporal attention [Su et al. 2024] to support variable-length sequences and a local attention window for long clips.

3.2.4 Motion decoding. The contextualized temporal feature h_t is decoded into both human motion and camera-related outputs:

$$\left(\theta_t^x, \beta_t, \Gamma_t^{GV}, \mathbf{v}_t^{root}, \Gamma_t^c, \tau_t^c, \mathbf{p}_t\right) = H(h_t). \tag{6}$$

To stabilize world-space motion, we optionally apply a contact-aware trajectory refinement following GVHMR [Shen et al. 2024a]. Given the predicted contact states, we optimize the root-translation velocity sequence by penalizing the world-space velocities of contact joints and high-frequency root jitter, and then integrate the refined velocities to recover the global root translation.

3.3 Close-Up-Aware Training

3.3.1 Adaptive close-up view augmentation. Real-world videos often contain close-up or upper-body framing, especially in livestream, vlog, and speech scenarios. Building on extreme-cropping augmentation in image-based HMR [Goel et al. 2023; Joo et al. 2021], we adapt this strategy to video using posture-aware crops that remain consistent across frames. Specifically, given the 2D body joints of a video clip, we adaptively crop the person based on an upper-body ratio:

$$r_{\text{up}} = \frac{d_{\text{head-hip}}}{h_{\text{body}}}, \tag{7}$$

where $d_{\text{head-hip}}$ represents the head-to-hip joint distance and h_{body} is the total visible height. For standing postures (higher r_{up}), the lower boundary is raised to prioritize the upper body, consistent with livestream and vlog-style framing. Conversely, for sitting postures (lower r_{up}), we preserve a larger lower-body region to prevent limb truncation. This pose-conditioned approach produces more realistic close-up views across diverse configurations than a fixed cropping strategy.

To further increase view diversity, we apply scale and translation perturbations to the crop, simulating different camera distances and off-center compositions. The perturbation is sampled at the clip level and shared by all frames, preserving temporal framing consistency and avoiding artificial crop jitter. Before resizing to the network input resolution, we apply a mild Gaussian blur when the crop is heavily downsampled to reduce aliasing artifacts. During training, we mix the synthesized close-up views with the original full-body views.

3.3.2 Partial hand observation modeling. Close-up view synthesis changes the visibility of hands: hands may remain fully visible, become partially truncated, shrink to a small region, or move outside the crop. We therefore recompute hand observations after view synthesis rather than reusing the original hand boxes.

For each hand, we define a visibility flag

$$v_h = \begin{cases} 1, & N_h \geq N_{\min} \text{ and } s_h \geq s_{\min}, \\ 0, & \text{otherwise}, \end{cases}$$

where N_h denotes the number of reliable visible hand keypoints inside the synthesized crop, and s_h is the resulting hand-box scale. A hand observation is treated as valid only when enough reliable keypoints remain visible, and the hand region is larger than a minimum hand box scale. Otherwise, the corresponding hand crop and hand-specific observations are masked. This prevents invalid hand crops or hallucinated detector outputs from being treated as reliable evidence.

This design exposes the model to realistic hand visibility conditions during training. When direct hand evidence is available, it can use local hand observations for detailed articulation. Otherwise, it learns to infer plausible hand motion from body context and temporal cues, matching real-world cases with occlusion, motion blur, and out-of-frame hands.

3.4 Training Objectives and Curriculum

We train the model with a compact SMPL-X reconstruction objective and introduce three task-specific designs for video whole-body recovery: hand-emphasized supervision, curriculum training, and visibility-aware hand supervision.

3.4.1 Hand emphasis. Applying a uniform loss across all SMPL-X joints is suboptimal for whole-body recovery. Body joints typically exhibit larger displacements than finger joints, causing body reconstruction errors to dominate the loss and leaving hand articulation weakly supervised. This imbalance is especially detrimental in close-up videos, where minor finger errors cause noticeably unnatural hand motions. We therefore re-weight hand pose and hand joint supervision, and additionally emphasize distal and fingertip joints:

$$\mathcal{L}_{tip} = \sum_{t} \sum_{j \in \mathcal{T}} \|\mathbf{J}_{t,j} - \hat{\mathbf{J}}_{t,j}\|_1, \tag{8}$$

where $\mathcal{T}$ denotes distal and fingertip joints. This fingertip-aware term directly constrains hand end-effectors, encouraging more accurate fine-grained articulation while preserving the full SMPL-X reconstruction objective.

3.4.2 Curriculum training. The training data contains heterogeneous supervision: large-scale body-centric videos provide broad motion coverage, while hand-rich whole-body data provides more detailed hand articulation. Training with a single uniform schedule can bias the model toward dominant body signals and underemphasize fine-grained hand motion. We therefore adopt a two-stage curriculum.

Stage I: General prior learning. In the first stage, we train on the full data mixture with the standard SMPL-X reconstruction objective and temporal regularization. This stage aims to learn stable body motion, coarse hand pose, camera-space reconstruction, and gravity-aware global motion. The goal is to establish a broad whole-body motion prior before focusing on fine hand details.

Stage II: Hand refinement. In the second stage, we increase the sampling ratio of high-quality hand and whole-body data, and strengthen the supervision on hand joints, especially distal and fingertip joints. Body and temporal supervision remain active during this stage to preserve whole-body consistency. This curriculum separates two learning objectives with different data requirements: diverse video data is used to learn robust body and global motion priors, while the later hand-focused stage refines the local articulation that is most important for visual quality.

3.4.3 Visibility-aware supervision. Real-world hand observations are frequently compromised by blur, occlusion, or truncation, causing 2D detectors to predict erroneous keypoints. Directly supervising these noisy inputs degrades temporal hand recovery. We therefore apply the hand reprojection loss only to reliable 2D hand observations. Specifically, each detected hand keypoint is assigned

a validity weight based on its detection confidence:

$$\mathcal{L}_{vis} = \frac{1}{\sum_{t,j} w_{t,j}} \sum_{t,j} w_{t,j} \left\| \Pi(\mathbf{J}_{t,j}) - \hat{\mathbf{x}}_{t,j} \right\|_1 . \tag{9}$$

Here, Π denotes camera projection, $\hat{\mathbf{x}}_{t,j}$ is the detected 2D hand keypoint, and $w_{t,j}$ is the validity weight derived from the detector confidence. We additionally discard hand crops with too few reliable keypoints or extremely small box sizes. Masking unreliable observations prevents noisy data from degrading training, allowing the temporal model to infer plausible hand motion from body context and adjacent valid frames.

4 Experiments

4.1 Experimental Setup

4.1.1 Datasets. We train our model on a mixture of motion capture, synthetic, and in-the-wild video datasets, including BEDLAM [Black et al. 2023], MOYO [Tripathi et al. 2023], ARCTIC [Fan et al. 2023], EgoBody [Zhang et al. 2022], AMASS [Mahmood et al. 2019], WHAC-A-Mole [Yin et al. 2024], 3DPW [Von Marcard et al. 2018], and Human3.6M [Ionescu et al. 2013]. To improve robustness to close-up and truncated videos, we apply close-up augmentation to BEDLAM, EgoBody, WHAC-A-Mole, and ARCTIC by simulating upper-body and partial-body crops. In the second training stage, we remove 3DPW, Human3.6M, and AMASS, and place greater emphasis on high-quality SMPL-X and hand-centric datasets for fine-grained whole-body reconstruction.

For evaluation, we consider two categories of benchmarks. We first evaluate whole-body results on ARCTIC [Fan et al. 2023] and UBody [Lin et al. 2023] datasets. ARCTIC is a controlled multi-view hand-object interaction dataset with accurate SMPL-X annotations, making it well-suited for evaluating articulated hand reconstruction and body-hand coordination. UBody contains diverse in-the-wild upper-body videos, including vlogs, video conferences, and sign language videos, in which severe truncation and expressive hand gestures pose significant challenges for whole-body recovery. We further report body-only reconstruction results on standard video HMR benchmarks, including 3DPW and EMDB. We follow the ARCTIC Protocol 1, UBody intra-scene split, and the official 3DPW training and test splits.

4.1.2 Metrics. For SMPL-X whole-body datasets, we report metrics for both the whole body and the hands, including PA-PVE, PVE, and PA-MPJPE. PA-PVE measures the Procrustes-aligned vertex error, PVE measures the raw vertex error, and PA-MPJPE measures the Procrustes-aligned joint error. These reconstruction errors are reported in millimeters (mm). For body-only video HMR benchmarks, we evaluate their body reconstruction errors.

To further evaluate temporal motion quality, we report MPJVE, Accel, and Jitter, which correspond to the errors in the first-, second-, and third-order temporal derivatives of the 3D joints, measured in mm/s, m/s^2, and m/s^3, respectively. MPJVE and Accel measure velocity and acceleration deviations from the ground truth, and Jitter quantifies the temporal instability of the motion. These metrics complement static frame-wise evaluations by capturing motion dynamics, acceleration consistency, and frame-to-frame smoothness. All reported metrics exclude trajectory refinement, which is applied only to the world-space results shown in the video.

4.1.3 Implementation details. We use HMR2.0 [Goel et al. 2023] and HaMeR [Pavlakos et al. 2024] as the frozen body and hand image feature extractors, respectively. We use ViTPose [Xu et al. 2024] and RTMW [Jiang et al. 2023, 2024] to extract 2D body and hand keypoints. YOLOv8 [Varghese and Sambath 2024] is used for detection. During training, all external detectors and feature extractors are kept frozen, and only our temporal reconstruction network is optimized. Hand keypoints with confidence lower than 0.55 are masked out. For close-up augmented samples, we recompute hand boxes after cropping and discard a hand observation if fewer than 5 valid hand keypoints remain visible or if the hand box scale is smaller than 20 pixels. The temporal window size is 120. We train the model in two stages. Stage I uses the full mixed training set for 207k steps. Stage II runs for another 88k steps, with increased sampling of high-quality SMPL-X and hand-centric data.

4.2 Whole-Body Reconstruction.

4.2.1 Quantitative results. Table 1 reports whole-body reconstruction results on ARCTIC and UBody. ARCTIC emphasizes articulated hand motion in hand-object interaction, and UBody focuses more on in-the-wild upper-body videos with truncation and expressive gestures. Consequently, these benchmarks serve to evaluate the hand reconstruction fidelity and the robustness of the proposed method in close-up whole-body recovery scenarios, respectively. On the ARCTIC dataset, the proposed method outperforms existing approaches across all reported hand metrics. Specifically, compared to the previous state-of-the-art, SMPLest-X, our approach achieves a 28.6% reduction in hand PA-PVE and a 13.9% reduction in hand PVE. Similarly, our method attains the lowest hand PVE on UBody. These quantitative improvements demonstrate that temporal body-hand modeling significantly enhances reconstruction accuracy in both controlled interaction settings and challenging, unconstrained video environments.

Notably, our trainable reconstruction network contains only about 46M trainable parameters, compared with 103M, 327M, and 687M for SMPLer-X-B, SMPLer-X-L, and SMPLest-X, respectively, while achieving competitive whole-body accuracy and substantially better hand reconstruction. This parameter efficiency stems from reusing strong frozen body and hand visual priors and concentrating the trainable capacity on the challenges specific to video whole-body recovery. Frozen body and hand encoders provide strong visual priors, while part-specific hand observations preserve local evidence that would otherwise be diluted by body-level features. Residual body-hand fusion integrates this evidence into a stable body-anchored representation, and the close-up-aware, hand-focused training further emphasizes challenging visibility and articulation cases.

4.2.2 Qualitative results. Fig. 3 presents qualitative comparisons on UBody and ARCTIC. Our method shows clear advantages over the image-based baseline SMPLest-X in half-body and hand-centric scenarios. In cases where a hand is outside the visible image region, SMPLest-X still tends to hallucinate implausible hand poses,

Table 1. Quantitative comparison of whole-body reconstruction on ARCTIC [Fan et al. 2023] and UBody [Lin et al. 2023]. The best performance is in boldface, and the second best is underlined.

Method	ARCTIC [Fan et al. 2023]						UBody [Lin et al. 2023]					
	PA-PVE ↓		PVE ↓		PA-MPJPE ↓		PA-PVE ↓		PVE ↓		PA-MPJPE ↓	
	All	Hands	All	Hands	All	Hands	All	Hands	All	Hands	All	Hands
PIXIE [Feng et al. 2021]	–	–	–	–	–	–	61.7	12.2	168.4	55.6	66.8	12.3
Hand4Whole [Moon et al. 2022]	63.4	18.1	136.8	54.8	–	–	44.8	8.9	104.1	45.7	45.5	9.0
OSX [Lin et al. 2023]	33.0	18.8	58.4	39.4	–	–	42.4	10.8	92.4	47.7	42.9	11.0
PyMAF-X [Zhang et al. 2023]	49.4	14.3	70.5	45.1	56.7	15.6	–	–	–	–	–	–
SMPLer-X-B [Cai et al. 2024]	54.0	17.9	85.2	53.4	55.1	18.4	35.5	11.0	65.3	46.9	37.2	10.9
SMPLer-X-L [Cai et al. 2024]	46.9	18.1	76.9	50.8	47.3	17.8	33.2	10.6	61.5	43.3	36.6	10.5
AiOS [Sun et al. 2024]	30.2	19.2	47.1	38.3	–	–	32.5	**7.3**	**58.6**	39.0	–	–
SMPLest-X [Yin et al. 2026]	**26.3**	11.9	**43.5**	28.8	–	–	31.6	9.5	59.8	37.7	–	–
GVHMR [Shen et al. 2024a]+HaMeR [Pavlakos et al. 2024]	41.0	13.9	71.0	54.6	55.1	11.7	–	–	–	–	–	–
Ours	28.1	**8.5**	44.7	**24.8**	**29.8**	**8.1**	**31.3**	7.4	61.0	**22.2**	**34.6**	**4.8**

Table 2. Quantitative comparison of body-only reconstruction on 3DPW [Von Marcard et al. 2018] and EMDB [Kaufmann et al. 2023].

Method	PA-MPJPE ↓	MPJPE ↓	PVE ↓	Accel ↓
3DPW [Von Marcard et al. 2018]				
GVHMR [Shen et al. 2024a]	37.0	56.6	68.7	5.2
GENMO [Li et al. 2025]	**34.6**	53.9	65.8	5.2
PromptHMR-Vid [Wang et al. 2025]	35.5	56.9	67.3	–
OSX [Lin et al. 2023]	60.6	86.2	–	–
SMPLer-X-B [Cai et al. 2024]	53.4	80.3	90.3	–
Multi-HMR [Baradel et al. 2024]	41.7	61.4	75.9	–
SMPLest-X [Yin et al. 2026]	43.2	70.5	–	–
Ours	35.2	**53.6**	**65.1**	**4.9**
EMDB [Kaufmann et al. 2023]				
GVHMR [Shen et al. 2024a]	44.5	74.2	85.9	3.9
GENMO [Li et al. 2025]	42.5	73.0	84.8	3.8
PromptHMR-Vid [Wang et al. 2025]	**40.1**	68.1	79.2	–
DUOMO [Wang et al. 2026]	41.8	67.1	78.2	–
Multi-HMR [Baradel et al. 2024]	50.1	81.6	95.7	–
Ours	**40.1**	**64.3**	**75.4**	**3.5**

as shown in cases (b), (e), and (f). By contrast, our method produces more reasonable predictions and avoids such spurious hand reconstructions. Our approach is also more robust under challenging conditions, such as hand occlusion (cases (d), (g), and (h)) and motion blur (cases (b) and (f)), where it still recovers plausible hand poses and coherent body-hand articulation. We attribute these improvements to our joint temporal modeling of body and hands, which allows the model to leverage temporal context and body motion cues to stabilize hand reconstruction. In contrast, the frame-wise image-based baseline lacks temporal reasoning and therefore yields noticeably less reliable hand predictions.

4.3 Body-Only Evaluation

Table 2 reports the comparison on standard body-only video HMR benchmarks, including 3DPW and EMDB. We compare our method with both video-based body-only methods and recent whole-body models. Even though our model is designed for whole-body SMPL-X reconstruction, it achieves state-of-the-art body reconstruction performance on both datasets, showing that our method preserves strong body pose accuracy. Compared with the strongest prior method DUOMO [Wang et al. 2026], our method reduces MPJPE by 4.2% on the EMDB benchmark. These results demonstrate that our method achieves state-of-the-art body-only reconstruction while additionally supporting temporally coherent whole-body and hand recovery.

4.4 Temporal Motion Quality

Table 3 evaluates temporal consistency on ARCTIC using Jitter, Accel, and MPJVE. These metrics measure complementary aspects of motion stability: Jitter reflects high-frequency temporal fluctuation, Accel measures acceleration-level motion error, and MPJVE evaluates velocity consistency with the ground-truth motion.

Image-based whole-body methods, such as SMPLer-X and SMPLest-X, suffer from severe temporal inconsistency because they reconstruct each frame independently. In contrast, GVHMR+HaMeR provides a much stronger baseline by combining a video-based body model with an image-based hand estimator, leading to significantly lower temporal errors than purely image-based methods. However, since the hands are still estimated independently by HaMeR and then stitched to the body, this pipeline cannot fully ensure temporally coherent body-hand motion. In contrast, our method predicts body and hands jointly in a temporal framework, leading to more stable whole-body motion and significantly smoother hand trajectories. Compared with GVHMR+HaMeR, our method reduces hand Jitter by 43.2% and hand MPJVE by 32.8%, demonstrating the benefit of joint temporal body-hand modeling.

4.5 Ablation Study

As shown in Table 4, we conduct ablation studies to validate the core architectural and training designs of our framework. We evaluate five variants on ARCTIC, focusing on both overall reconstruction quality and hand-centric performance. Specifically, (1) replaces our residual body-hand fusion with early fusion of all features, (2) removes part-specific hand observations and relies mainly on body-level cues, (3) disables close-up view augmentation during training, (4) removes the second-stage hand-focused training, and (5) removes the visibility-aware hand supervision term $\mathcal{L}_{vis}$.

The comparison shows that each design contributes to hand reconstruction quality and temporal stability. Variant (1) verifies the importance of structured body-hand fusion: directly compressing all

Table 3. Temporal stability comparison on ARCTIC [Fan et al. 2023]. Lower values indicate smoother and more accurate temporal motion.

Method	All			Hands		
	Jitter ↓	Accel ↓	MPJVE ↓	Jitter ↓	Accel ↓	MPJVE ↓
SMPLer-X-B [Cai et al. 2024]	127.5	23.8	482.6	52.1	9.9	219.9
SMPLest-X [Yin et al. 2026]	95.1	17.8	364.6	55.4	10.4	228.5
GVHMR [Shen et al. 2024a]+HaMeR [Pavlakos et al. 2024]	6.0	1.8	109.0	7.4	1.6	100.7
Ours	5.4	1.5	81.3	4.2	1.5	67.7

Table 4. Ablation study on ARCTIC [Fan et al. 2023]. We report whole-body (All) PVE to measure overall whole-body reconstruction quality, and Hand PA-PVE, Hand PVE, and Hand Jitter to evaluate hand accuracy and temporal stability.

Variant	ARCTIC [Fan et al. 2023]			
	All PVE ↓	Hand PA-PVE ↓	Hand PVE ↓	Hand Jitter ↓
Ours	44.7	8.5	24.8	4.2
(1) w/o Res fusion	49.2	9.4	28.2	6.6
(2) w/o Hand obs.	55.2	15.8	44.8	10.1
(3) w/o Close-up aug.	48.4	9.2	31.1	5.9
(4) w/o Two-stage	49.9	10.5	31.7	4.8
(5) w/o $\mathcal{L}_{vis}$	46.1	9.3	27.3	5.7

body and hand features through early fusion weakens the interaction between global body context and local hand evidence, leading to degraded hand accuracy and jitter. Variant (2) produces a clear drop in hand-related metrics, confirming that body-level observations alone are insufficient for fine-grained hand articulation and that part-specific hand cues are essential. Variant (3) mainly affects robustness, where upper-body framing, truncation, and hand entry/exit are common, demonstrating the benefit of close-up augmentation for in-the-wild videos. Variant (4) shows that the second-stage training further improves hand reconstruction by emphasizing high-quality SMPL-X and hand-centric data. Finally, variant (5) highlights the importance of visibility-aware supervision: without masking invisible or unreliable hand regions, noisy supervision from occluded or out-of-frame hands harms both hand accuracy and temporal stability. Overall, the full model consistently achieves the best balance between whole-body accuracy, hand reconstruction quality, and temporal smoothness.

4.6 Qualitative Results on Real-World Videos

Fig. 5 shows qualitative results on challenging in-the-wild internet videos. Our method produces stable and coherent whole-body motion across diverse scenarios, including agile hand interactions, severe motion blur, and complex body movements. Fig. 4 shows a challenging close-up video with frequent hand truncation. Compared with the image-based SMPLest-X baseline, our method produces significantly more stable and temporally coherent hand motion under partial visibility. More qualitative results can be found in the supplementary video.

4.7 Computational Cost

We evaluate runtime on a 312-frame static-camera video using an RTX 6000 Ada GPU. In our sequential pipeline, YOLOv8 detection, ViTPose, RTMW, HMR2.0 feature extraction, and HaMeR feature extraction require 6.74, 8.14, 8.80, 4.34, and 10.83 seconds, respectively, while the DanceHMR network takes only 0.03 seconds. The full pipeline processes the video in 38.9 seconds, corresponding to 124.6 ms per frame or 8.0 FPS, compared with 15.5 FPS for GVHMR under the same setting. Its total computational cost is 1.55 TFLOPs per frame, of which DanceHMR contributes only 0.10 GFLOPs. Thus, the proposed temporal reconstruction network adds negligible overhead, while the end-to-end runtime is dominated by the frozen visual front-ends.

Although the reconstruction network is computationally lightweight, it uses bidirectional attention over 120-frame windows and is therefore designed for offline processing. Extending it to causal streaming with masked temporal attention and a rolling feature window is left for future work.

5 Conclusion

In this paper, we presented DanceHMR, a temporally coherent body and hand human mesh recovery framework for monocular videos. Our method jointly models body motion and hand articulation through residual body-hand fusion within a unified temporal architecture, and improves robustness with close-up-aware augmentation. Experiments demonstrate improved hand reconstruction, competitive body accuracy, and stable SMPL-X motion in challenging real-world videos.

References

Fabien Baradel, Matthieu Armando, Salma Galaaoui, Romain Brégier, Philippe Weinzaepfel, Grégory Rogez, and Thomas Lucas. 2024. Multi-hmr: Multi-person whole-body human mesh recovery in a single shot. In *European Conference on Computer Vision*. Springer, 202–218.

Michael J Black, Priyanka Patel, Joachim Tesch, and Jinlong Yang. 2023. Bedlam: A synthetic dataset of bodies exhibiting detailed lifelike animated motion. In *Proceedings of the IEEE/CVF Conference on Computer Vision and Pattern Recognition*. 8726–8737.

Zhongang Cai, Wanqi Yin, Ailing Zeng, Chen Wei, Qingping Sun, Wang Yanjun, Hui En Pang, Haiyi Mei, Mingyuan Zhang, Lei Zhang, et al. 2024. Smpler-x: Scaling up expressive human pose and shape estimation. *Advances in Neural Information Processing Systems* 36 (2024).

Yue Chen, Xingyu Chen, Yuxuan Xue, Anpei Chen, Yuliang Xiu, and Pons-Moll Gerard. 2025. Human3R: Everyone Everywhere All at Once. *arXiv preprint arXiv:2510.06219* (2025).

Hongsuk Choi, Gyeongsik Moon, Ju Yong Chang, and Kyoung Mu Lee. 2021. Beyond static features for temporally consistent 3d human pose and shape from a video. In *Proceedings of the IEEE/CVF conference on computer vision and pattern recognition*. 1964–1973.

Vasileios Choutas, Georgios Pavlakos, Timo Bolkart, Dimitrios Tzionas, and Michael J Black. 2020. Monocular expressive body regression through body-driven attention. In *Computer Vision–ECCV 2020: 16th European Conference, Glasgow, UK, August 23–28, 2020, Proceedings, Part X 16*. Springer, 20–40.

Zicong Fan, Omid Taheri, Dimitrios Tzionas, Muhammed Kocabas, Manuel Kaufmann, Michael J Black, and Otmar Hilliges. 2023. ARCTIC: A dataset for dexterous bimanual hand-object manipulation. In *Proceedings of the IEEE/CVF Conference on Computer Vision and Pattern Recognition*. 12943–12954.

Yao Feng, Vasileios Choutas, Timo Bolkart, Dimitrios Tzionas, and Michael J Black. 2021. Collaborative regression of expressive bodies using moderation. In *2021 International Conference on 3D Vision (3DV)*. IEEE, 792–804.

Shubham Goel, Georgios Pavlakos, Jathushan Rajasegaran, Angjoo Kanazawa, and Jitendra Malik. 2023. Humans in 4d: Reconstructing and tracking humans with transformers. In *Proceedings of the IEEE/CVF International Conference on Computer Vision*. 14783–14794.

Catalin Ionescu, Dragos Papava, Vlad Olaru, and Cristian Sminchisescu. 2013. Human3. 6m: Large scale datasets and predictive methods for 3d human sensing in natural environments. *IEEE transactions on pattern analysis and machine intelligence* 36, 7 (2013), 1325–1339.

Tao Jiang, Peng Lu, Li Zhang, Ningsheng Ma, Rui Han, Chengqi Lyu, Yining Li, and Kai Chen. 2023. RTMPose: Real-Time Multi-Person Pose Estimation based on MMPose. doi:10.48550/ARXIV.2303.07399

Tao Jiang, Xinchen Xie, and Yining Li. 2024. RTMW: Real-Time Multi-Person 2D and 3D Whole-body Pose Estimation. *arXiv preprint arXiv:2407.08634* (2024).

Hanbyul Joo, Natalia Neverova, and Andrea Vedaldi. 2021. Exemplar fine-tuning for 3d human model fitting towards in-the-wild 3d human pose estimation. In *2021 International Conference on 3D Vision (3DV)*. IEEE, 42–52.

Manuel Kaufmann, Jie Song, Chen Guo, Kaiyue Shen, Tianjian Jiang, Chengcheng Tang, Juan José Zárate, and Otmar Hilliges. 2023. EMDB: The Electromagnetic Database of Global 3D Human Pose and Shape in the Wild. In *International Conference on Computer Vision (ICCV)*.

Muhammed Kocabas, Nikos Athanasiou, and Michael J Black. 2020. Vibe: Video inference for human body pose and shape estimation. In *Proceedings of the IEEE/CVF conference on computer vision and pattern recognition*. 5253–5263.

Jiefeng Li, Jinkun Cao, Haotian Zhang, Davis Rempe, Jan Kautz, Umar Iqbal, and Ye Yuan. 2025. GENMO: A GENeralist Model for Human MOtion. In *Proceedings of the IEEE/CVF International Conference on Computer Vision (ICCV)*.

Jing Lin, Ailing Zeng, Haoqian Wang, Lei Zhang, and Yu Li. 2023. One-stage 3d whole-body mesh recovery with component aware transformer. In *Proceedings of the IEEE/CVF Conference on Computer Vision and Pattern Recognition*. 21159–21168.

Naureen Mahmood, Nima Ghorbani, Nikolaus F Troje, Gerard Pons-Moll, and Michael J Black. 2019. AMASS: Archive of motion capture as surface shapes. In *Proceedings of the IEEE/CVF international conference on computer vision*. 5442–5451.

Gyeongsik Moon, Hongsuk Choi, and Kyoung Mu Lee. 2022. Accurate 3D hand pose estimation for whole-body 3D human mesh estimation. In *Proceedings of the IEEE/CVF Conference on Computer Vision and Pattern Recognition*. 2308–2317.

Georgios Pavlakos, Dandan Shan, Ilija Radosavovic, Angjoo Kanazawa, David Fouhey, and Jitendra Malik. 2024. Reconstructing hands in 3d with transformers. In *Proceedings of the IEEE/CVF Conference on Computer Vision and Pattern Recognition*. 9826–9836.

Rolandos Alexandros Potamias, Jinglei Zhang, Jiankang Deng, and Stefanos Zafeiriou. 2025. Wilor: End-to-end 3d hand localization and reconstruction in-the-wild. In *Proceedings of the Computer Vision and Pattern Recognition Conference*. 12242–12254.

Davis Rempe, Tolga Birdal, Aaron Hertzmann, Jimei Yang, Srinath Sridhar, and Leonidas J Guibas. 2021. Humor: 3d human motion model for robust pose estimation. In *Proceedings of the IEEE/CVF international conference on computer vision*. 11488–11499.

Wenhao Shen, Hao Wang, Wanqi Yin, Fayao Liu, Xulei Yang, Chao Liang, Zhongang Cai, and Guosheng Lin. 2026. VLM-Guided Group Preference Alignment for Diffusion-based Human Mesh Recovery. In *Proceedings of the IEEE/CVF Conference on Computer Vision and Pattern Recognition (CVPR)*. 13918–13929.

Wenhao Shen, Wanqi Yin, Hao Wang, Chen Wei, Zhongang Cai, Lei Yang, and Guosheng Lin. 2024b. HMR-Adapter: A Lightweight Adapter with Dual-Path Cross Augmentation for Expressive Human Mesh Recovery. In *Proceedings of the 32nd ACM International Conference on Multimedia*. 6093–6102.

Wenhao Shen, Wanqi Yin, Xiaofeng Yang, Cheng Chen, Chaoyue Song, Zhongang Cai, Lei Yang, Hao Wang, and Guosheng Lin. 2025. ADHMR: aligning diffusion-based human mesh recovery via direct preference optimization. In *Proceedings of the 42nd International Conference on Machine Learning* (Vancouver, Canada) *(ICML'25)*. JMLR.org, Article 2169, 12 pages.

Xiaolong Shen, Zongxin Yang, Xiaohan Wang, Jianxin Ma, Chang Zhou, and Yi Yang. 2023. Global-to-local modeling for video-based 3d human pose and shape estimation. In *Proceedings of the IEEE/CVF Conference on Computer Vision and Pattern Recognition*. 8887–8896.

Zehong Shen, Huaijin Pi, Yan Xia, Zhi Cen, Sida Peng, Zechen Hu, Hujun Bao, Ruizhen Hu, and Xiaowei Zhou. 2024a. World-grounded human motion recovery via gravity-view coordinates. In *SIGGRAPH Asia 2024 Conference Papers*. 1–11.

Soyong Shin, Juyong Kim, Eni Halilaj, and Michael J Black. 2024. Wham: Reconstructing world-grounded humans with accurate 3d motion. In *Proceedings of the IEEE/CVF Conference on Computer Vision and Pattern Recognition*. 2070–2080.

Jianlin Su, Murtadha Ahmed, Yu Lu, Shengfeng Pan, Wen Bo, and Yunfeng Liu. 2024. Roformer: Enhanced transformer with rotary position embedding. *Neurocomputing* 568 (2024), 127063.

Qingping Sun, Yanjun Wang, Ailing Zeng, Wanqi Yin, Chen Wei, Wenjia Wang, Haiyi Mei, Chi-Sing Leung, Ziwei Liu, Lei Yang, et al. 2024. Aios: All-in-one-stage expressive human pose and shape estimation. In *Proceedings of the IEEE/CVF conference on computer vision and pattern recognition*. 1834–1843.

Yu Sun, Qian Bao, Wu Liu, Tao Mei, and Michael J Black. 2023. Trace: 5d temporal regression of avatars with dynamic cameras in 3d environments. In *Proceedings of the IEEE/CVF Conference on Computer Vision and Pattern Recognition*. 8856–8866.

Shashank Tripathi, Lea Müller, Chun-Hao P. Huang, Taheri Omid, Michael J. Black, and Dimitrios Tzionas. 2023. 3D Human Pose Estimation via Intuitive Physics. In *Conference on Computer Vision and Pattern Recognition (CVPR)*. 4713–4725. https://ipman.is.tue.mpg.de

Rejin Varghese and M Sambath. 2024. Yolov8: A novel object detection algorithm with enhanced performance and robustness. In *2024 International conference on advances in data engineering and intelligent computing systems (ADICS)*. IEEE, 1–6.

Timo Von Marcard, Roberto Henschel, Michael J Black, Bodo Rosenhahn, and Gerard Pons-Moll. 2018. Recovering accurate 3d human pose in the wild using imus and a moving camera. In *Proceedings of the European conference on computer vision (ECCV)*. 601–617.

Yufu Wang, Evonne Ng, Soyong Shin, Rawal Khirodkar, Yuan Dong, Zhaoen Su, Jinhyung Park, Kris Kitani, Alexander Richard, Fabian Prada, and Michael Zollhofer. 2026. DuoMo: Dual Motion Diffusion for World-Space Human Reconstruction. *arXiv preprint arXiv:2603.03265* (2026).

Yufu Wang, Yu Sun, Priyanka Patel, Kostas Daniilidis, Michael J Black, and Muhammed Kocabas. 2025. Prompthmr: Promptable human mesh recovery. In *Proceedings of the computer vision and pattern recognition conference*. 1148–1159.

Yufu Wang, Ziyun Wang, Lingjie Liu, and Kostas Daniilidis. 2024. Tram: Global trajectory and motion of 3d humans from in-the-wild videos. In *European Conference on Computer Vision*. Springer, 467–487.

Wen-Li Wei, Jen-Chun Lin, Tyng-Luh Liu, and Hong-Yuan Mark Liao. 2022. Capturing humans in motion: Temporal-attentive 3d human pose and shape estimation from monocular video. In *Proceedings of the IEEE/CVF Conference on Computer Vision and Pattern Recognition*. 13211–13220.

Jiahao Wu, Yunfei Liu, Lijian Lin, Ye Zhu, Lei Zhu, Jingyi Li, and Yu Li. 2026. PEAR: Pixel-aligned Expressive humAn mesh Recovery. In *Proceedings of the Special Interest Group on Computer Graphics and Interactive Techniques Conference Conference Papers (SIGGRAPH Conference Papers '26)*. Association for Computing Machinery, New York, NY, USA, Article 46, 12 pages. doi:10.1145/3799902.3811096

Yufei Xu, Jing Zhang, Qiming Zhang, and Dacheng Tao. 2024. ViTPose++: Vision Transformer Foundation Model for Generic Body Pose Estimation. *IEEE Transactions on Pattern Analysis and Machine Intelligence* 46 (2024), 1212–1230. doi:10.1109/TPAMI.2023.3330016

Vickie Ye, Georgios Pavlakos, Jitendra Malik, and Angjoo Kanazawa. 2023. Decoupling human and camera motion from videos in the wild. In *Proceedings of the IEEE/CVF conference on computer vision and pattern recognition*. 21222–21232.

Wanqi Yin, Zhongang Cai, Ruisi Wang, Fanzhou Wang, Chen Wei, Haiyi Mei, Weiye Xiao, Zhitao Yang, Qingping Sun, Atsushi Yamashita, et al. 2024. Whac: World-grounded humans and cameras. In *European Conference on Computer Vision*. Springer, 20–37.

Wanqi Yin, Zhongang Cai, Ruisi Wang, Ailing Zeng, Chen Wei, Qingping Sun, Haiyi Mei, Yanjun Wang, Hui En Pang, Mingyuan Zhang, Lei Zhang, Chen Change Loy, Atsushi Yamashita, Lei Yang, and Ziwei Liu. 2026. SMPLest-X: Ultimate Scaling for Expressive Human Pose and Shape Estimation . *IEEE Transactions on Pattern Analysis & Machine Intelligence* 48, 02 (Feb. 2026), 1778–1794. doi:10.1109/TPAMI.2025.3618174

Ye Yuan, Umar Iqbal, Pavlo Molchanov, Kris Kitani, and Jan Kautz. 2022. Glamr: Global occlusion-aware human mesh recovery with dynamic cameras. In *Proceedings of the IEEE/CVF conference on computer vision and pattern recognition*. 11038–11049.

Hongwen Zhang, Yating Tian, Yuxiang Zhang, Mengcheng Li, Liang An, Zhenan Sun, and Yebin Liu. 2023. Pymaf-x: Towards well-aligned full-body model regression from monocular images. *IEEE Transactions on Pattern Analysis and Machine Intelligence* (2023).

Jinglei Zhang, Jiankang Deng, Chao Ma, and Rolandos Alexandros Potamias. 2025. Hawor: World-space hand motion reconstruction from egocentric videos. In *Proceedings of the Computer Vision and Pattern Recognition Conference*. 1805–1815.

Siwei Zhang, Qianli Ma, Yan Zhang, Zhiyin Qian, Taein Kwon, Marc Pollefeys, Federica Bogo, and Siyu Tang. 2022. Egobody: Human body shape and motion of interacting people from head-mounted devices. In *European conference on computer vision*. Springer, 180–200.

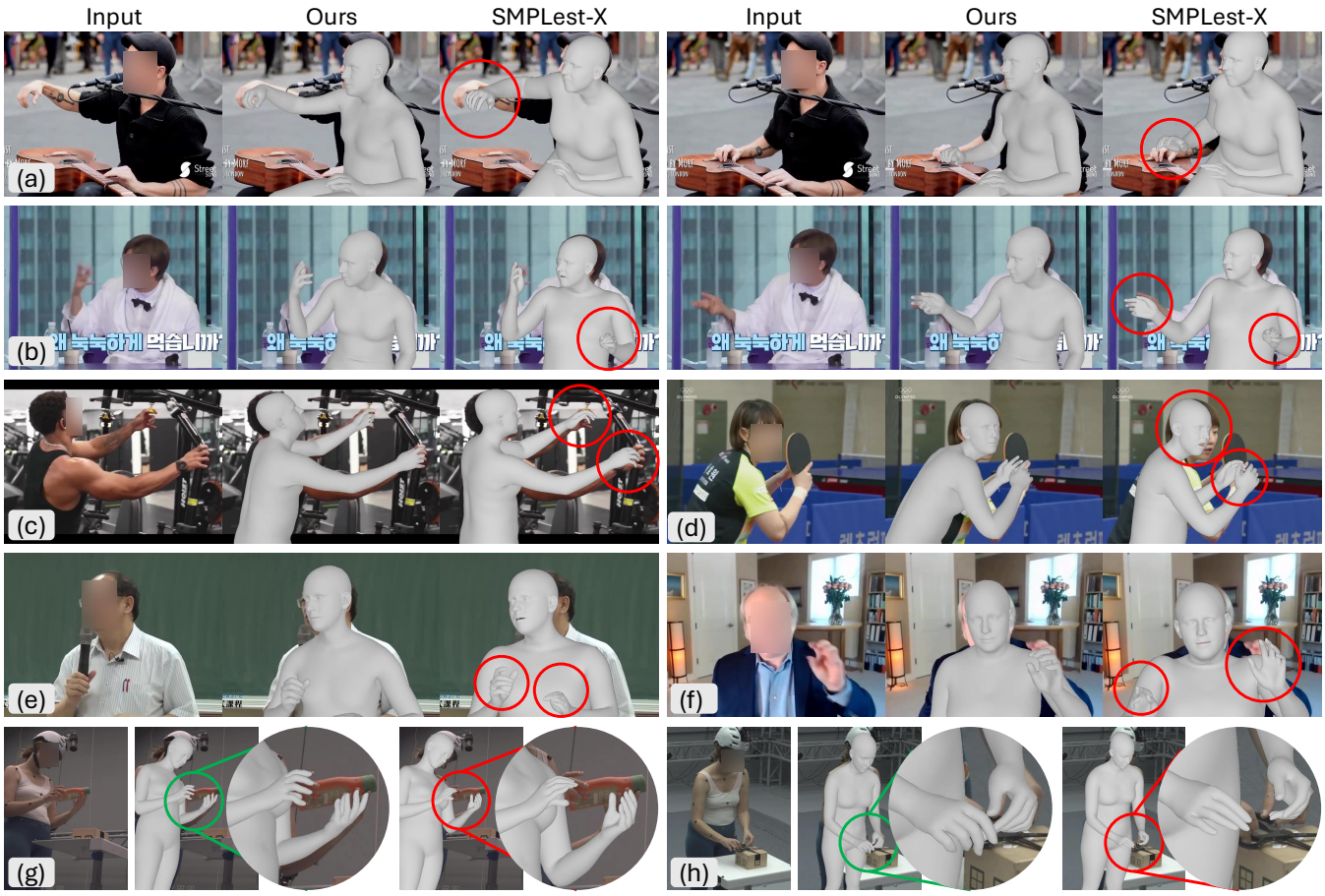

Fig. 3. Qualitative results on UBody [Lin et al. 2023] (a~f) and ARCTIC [Fan et al. 2023] (g~h). Compared with the image-based SMPLest-X [Yin et al. 2026] baseline, which often fails in close-up and partial-body scenes, especially for hand pose estimation, our method produces more stable and plausible body-hand reconstructions across diverse half-body and hand-centric scenarios. Please zoom in for better visualization.

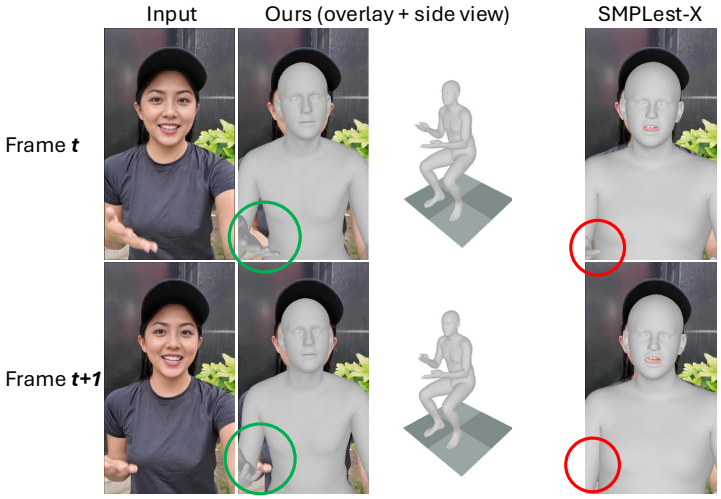

Fig. 4. Qualitative comparison on a close-up internet video with frequent hand truncation. Since the right hand repeatedly enters and leaves the frame, SMPLest-X produces inconsistent hand poses across neighboring frames, resulting in visible jitter. Our method recovers more natural and temporally coherent hand motion, while preserving plausible body poses.

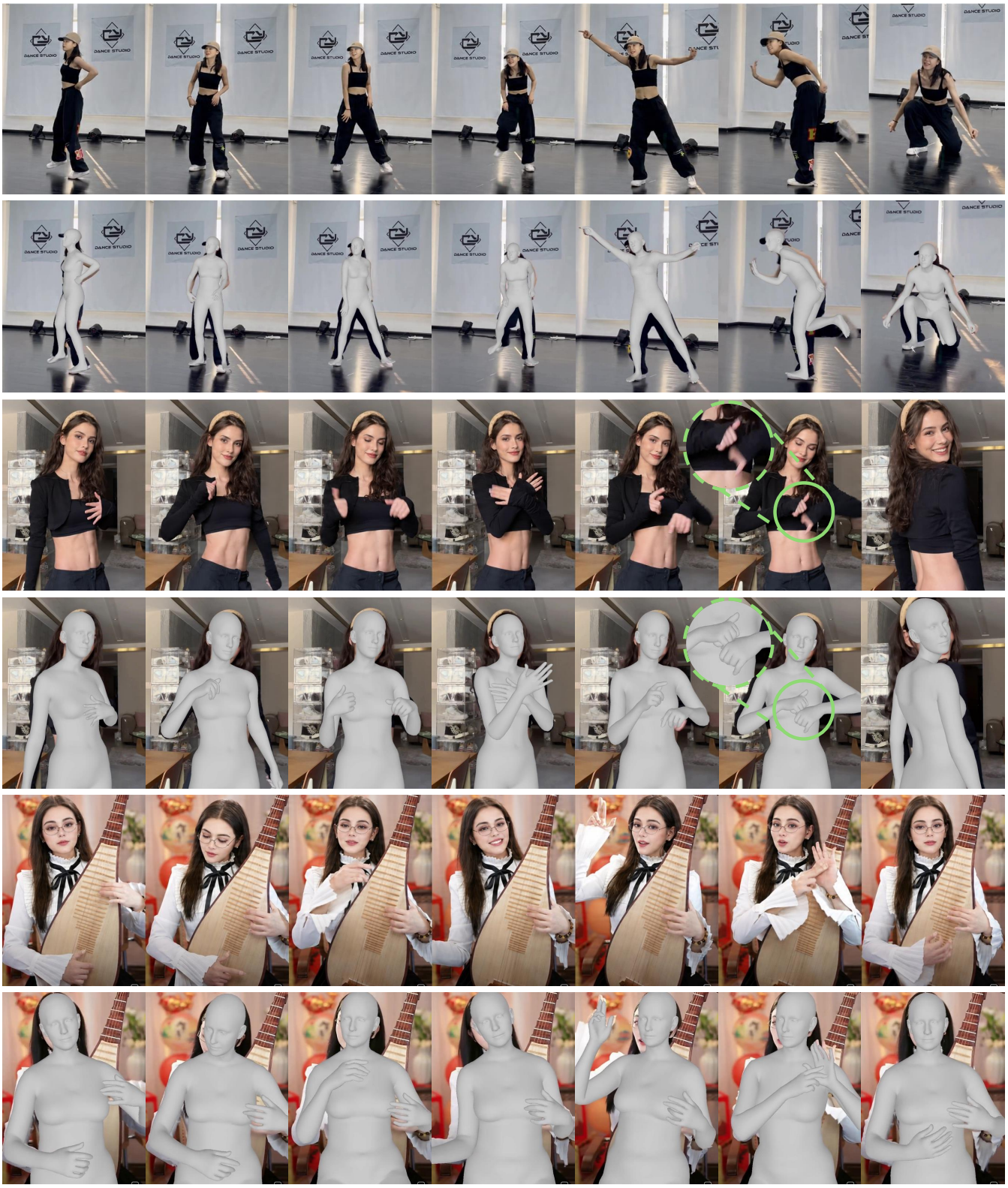

Fig. 5. Qualitative results of our DanceHMR on challenging in-the-wild internet videos. For each example, we show input video frames and our reconstructed SMPL-X overlay. DanceHMR recovers high-quality body and hand motion in fast dance, close-up, and livestream scenarios, maintaining stable hands and coherent whole-body dynamics. Please zoom in for better visualization.